

## Cluster-assisted multiple ionization of xenon and krypton by a nanosecond laser

Xiaolin Luo, Haiyang Li,\* Dongmei Niu, Lihua Wen, Feng Liang, Bin Wang, and Xue Xiao  
*Dalian Institute of Chemical Physics, Dalian, 116023 and Anhui Institute of Optics and Fine Mechanics, Hefei, 230031,  
 Chinese Academy of Sciences, People's Republic of China*

(Received 3 February 2005; published 26 July 2005)

Multicharged xenon and krypton ions with charge states up to  $\text{Xe}^{11+}$  and  $\text{Kr}^{11+}$  have been observed in laser ionization of a pulsed xenon or krypton beam by a 25 ns Nd-YAG laser with laser intensity of  $10^{10}$ – $10^{11}$   $\text{W cm}^{-2}$  at 532 nm. There is strong evidence to support that those multicharged ions come from cluster-assisted electron recolliding ionizations inside the cluster after multiphoton ionization of atoms in the cluster, the electron can gain its kinetic energy by inverse bremsstrahlung absorption from a laser field quickly.

DOI: [10.1103/PhysRevA.72.013201](https://doi.org/10.1103/PhysRevA.72.013201)

PACS number(s): 36.40.Gk, 42.50.Hz, 32.80.Fb

### I. INTRODUCTION

The interaction of atoms and atomic clusters, especially for rare gas atoms like xenon and krypton, with high-intensity laser pulses has been studied by a number of groups over the past few years [1–12]. Many investigations indicate that the photoionization behavior of clusters under a laser field has apparent discrepancies to that of atoms; even clusters of different sizes represent dissimilarities of ionization. When an atom is subjected to a strong laser field, multicharged ions are observed [8,9], but no kinetic energy of these ions has been reported even though the charge state is high up to +20 [9]. The kinetic energy of the product ions is expected to increase with the size of a system, being of the order of hundreds of eV in small clusters [10] and tens or hundreds of keV in large clusters, composed of  $n \sim 10^3$ – $10^5$  atoms [11,12]. Snyder reported cluster-assisted multiple ionization of a xenon and krypton cluster by a 624 nm femtosecond laser at a laser intensity  $10^{15}$   $\text{W cm}^{-2}$ , highly charged atomic species, e.g.,  $\text{Xe}^{20+}$ ,  $\text{Kr}^{18+}$  were observed [10]. Recently, Wabnitz *et al.* studied the multiple ionization of atomic clusters by intense soft x rays from a free electron laser, atomic ions with charges up to 8+ were detected when the xenon cluster was irradiated [7]. Zamith *et al.* carried out an optimal-control experiment on the production of highly charged ions in intense laser field irradiation of large xenon clusters [3]. Various models have been developed to explain these observations, including enhanced ionization model [1,2], molecular dynamics simulation method [13], ionization ignition model (IIM) [14], and “nanoplasma” model [15]. Common to these models, the initial ionization is tunnel ionization, and the atoms in a cluster are at least single ionized in a few femtoseconds in the rising edge of the laser pulse. Further ionization occurs via charge-assisted field ionization and electron impact (EI) ionization of atoms by energetic, laser-driven electrons inside the cluster [1,2,11–15].

Recently, we reported the production of  $\text{C}^{q+}$  ( $q=2,3$ ) and  $\text{I}^{q+}$  ( $q=2,3$ ) in photoionization of benzene or methyl iodide seeded in noble gas by 25 ns, 532 nm pulses at a laser inten-

sity of about  $10^{11}$   $\text{W cm}^{-2}$  [16–18], and found the existence of clusters in the beam was vital to produce those multiply charged ions. In fact, the generation of multicharged ions from molecules using a nanosecond laser is not a new phenomenon [19,20]. Armstrong *et al.* observed  $\text{U}^{q+}$  ( $q=1-4$ ) in the study of the laser ionization of  $\text{UF}_6$  using a Nd-YAG laser with a laser intensity of about  $10^9$ – $10^{13}$   $\text{W cm}^{-2}$  and proposed that the  $\text{U}^{q+}$  come from the dissociation of the highly excited molecule, superexcited  $\text{UF}_6^{**}$ , which is speculated to be facilitated by the “giant resonance.” But this “giant resonance” model is difficult to explain the role of cluster to the production of multicharged ions for molecules of quite different structures, for example  $\text{C}_6\text{H}_6$  and  $\text{CH}_3\text{I}$ .

In order to get more insight about the mechanism of cluster-assisted multiple ionization, atomic clusters should be used as the target for intense laser irradiation. In this work, we present the results of cluster-assisted laser multiple ionization of Xe and Kr at a laser intensity in the range of  $10^{10}$ – $10^{11}$   $\text{W cm}^{-2}$ , in which multicharged atomic ions with charge states up to  $\text{Xe}^{11+}$  and  $\text{Kr}^{11+}$  are produced. To the best of our knowledge, these are the highest charged ions produced under such laser intensity, which can provide some clues of coupling mechanisms between laser and atomic clusters.

### II. EXPERIMENT

The apparatus used in this study was a homemade two-stage linear time-of-flight (TOF) mass spectrometer, which has been described in detail previously [16]. Briefly, the xenon or krypton gas was expanded to the chamber via a pulsed nozzle (General Valve, diameter 0.5 mm) and then passed through a skimmer ( $d=3$  mm) to be irradiated by the 532 nm laser pulse (Spectron SL803, 25 ns) about 13 cm downstream of the valve nozzle. The intensity of the laser used in the experiment ranged from  $10^{10}$  to  $10^{11}$   $\text{W cm}^{-2}$  by adjusting the voltages of the pumping xenon lamp. The pressure was maintained at several  $10^{-4}$  Pa while running the experiment at 10 Hz. A needle valve was used to produce the effused beam, and the pressure in the ionization chamber was also kept at several  $10^{-4}$  Pa. The produced ions were detected by dual microchannel plates (MCP) after 500 mm field-free flight and recorded by a digital oscilloscope (Tek-

\*Corresponding author. Email address: hli@dicp.ac.cn

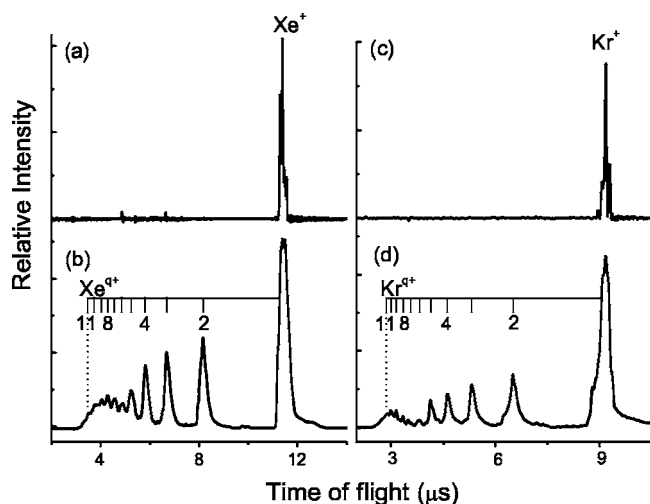


FIG. 1. Time-of-flight mass spectra of Xe and Kr irradiated by a 532 nm laser at an intensity of  $10^{11} \text{ W cm}^{-2}$ , (a) Xe effused beam; (b) 0.4 MPa Xe pulsed beam; (c) Kr effused beam; and (d) 0.4 MPa Kr pulsed beam.

tronix, TDS224), after averaging for 128 laser shots. The gas, Xe and Kr, purchased from Nanjing Special Gases Corporation, had a purity of 99.99% and had not been further purified.

### III. RESULT AND DISCUSSION

Figure 1 shows typical TOF mass spectra of Xe and Kr irradiated by a 532 nm laser at an intensity of  $10^{11} \text{ W cm}^{-2}$ . We can see the obvious differences between TOF spectra taken using an effused beam and a pulsed beam. When the effused beams of xenon and krypton were irradiated by a 532 nm laser, as shown in Figs. 1(a) and 1(c), only single charged ions appeared in the mass spectra, i.e.,  $\text{Xe}^+$  and  $\text{Kr}^+$ , and their isotopes were clearly resolved, which means their kinetic energies are small. While the pulsed atomic beam was used, multicharged ions of  $\text{Xe}^{q+}$  and  $\text{Kr}^{q+}$  ( $q=2-11$ ) can clearly be seen. Higher charged species may be present, but the broad isotope distribution of xenon and krypton do not allow for their unambiguous identification. The total intensities of multicharged ions in Figs. 1(b) and 1(d) are even higher than the integrated intensity of single charged ions, which imply extremely efficient coupling of the laser with the species in the beam. One should note that efficient production of  $\text{Xe}^{10+}$  and  $\text{Xe}^{11+}$  is of particular importance for the generation of soft x rays in the 11–13.5 nm range, where extreme ultraviolet lithography is developed [3,21].

The Keldysh parameter  $\gamma=(E_{IP}/2U_p)^{1/2}$  is widely used to judge the ionization mechanism, multiphoton ionization (MPI) or tunneling ionization [22]. Here,  $E_{IP}$  is the ionization potential of the atom,  $U_p=9.3 \times 10^{-14}I \text{ (W cm}^{-2}\text{)} \lambda^2(\mu\text{m})$  is the ponderomotive potential of the radiation field and refers to the quiver motion of the electron in the oscillating field,  $I$  is the laser intensity, and  $\lambda$  is the laser wavelength. If  $\gamma>1$ , MPI dominates the ionization process. The Keldysh parameters for single ionization of Xe and Kr atoms are calculated to be 25 even at the maximum intensity of 4

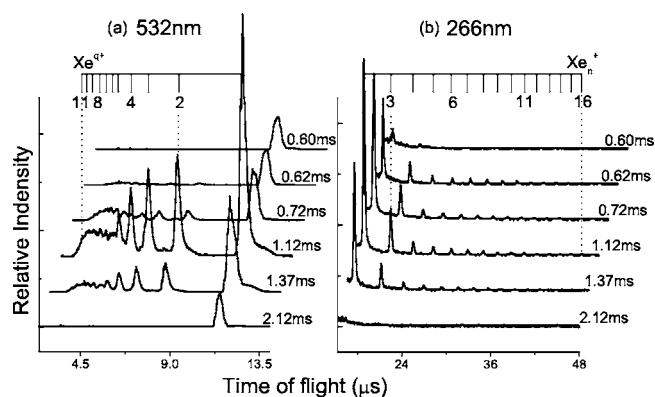


FIG. 2. Time-of-flight mass spectra of Xe by the interaction of different portions of a 0.4 MPa pulsed beam with (a) a 532 nm laser and (b) a 266 nm laser.

$\times 10^{11} \text{ W cm}^{-2}$  used in our experiment, so the initial ionization event starts from multiphoton ionization. The highly charged ions observed in Figs. 1(b) and 1(d) must come from some further ionization processes after multiphoton ionization of Xe/Kr atoms.

The most important difference between a jet beam and effused inlet is that a cluster may exist in the jet beam, so we speculate that multicharged ions appeared in the atomic beam experiment may come from ionization of an atomic cluster in the beam. Generally speaking, in a jet beam, the concentration of a larger cluster is the highest in the middle of the beam, while at the head and tail, the density of the cluster is much lower, and the clusters' size will augment rapidly with the increasing of the backing pressure of the gas. Actually the results in Figs. 1(b) and 1(d) were obtained at the middle part of the jet beam at the maximal backing pressure. Therefore two kinds of experiments were taken to confirm the contribution of clusters to the production of multicharged ions.

First, we adjusted the delay time between the laser and the pulsed valve and made the laser irradiating on different portions of the pulsed beam. Figures 2(a) and 2(b) display the mass spectra taken at different delay times by a 532 and 266 nm laser, respectively, xenon backing pressure was 0.4 MPa. The good consistency between the intensities of multicharged ions in Fig. 2(a) and the intensities of  $\text{Xe}_n^+$  cluster ions in Fig. 2(b) provide direct evidence that the large clusters in the beam play a very important role in the generation of the highly charged ions. The largest cluster observed was  $\text{Xe}_{16}^+$ , but the real size of the clusters in the dense portion of the pulsed Xe beam may be much larger due to laser-induced fragmentation of the cluster ions after MPI.

Second, TOF mass spectra in the dense portion of the pulsed beam were taken by varying the backing pressure of the valve, which are shown in Figs. 3(a) Xe and 3(b) Kr, respectively. As we can see, the intensities of multicharged ions increase quickly with the increasing of the backing pressures. The lowest backing pressures needed to produce multiple charged ions for xenon is 0.2 MPa, but the lowest backing pressure for krypton is 0.3 MPa. This could be due to that xenon is easier to form a cluster than krypton, which also supports the cluster-assisted hypothesis.

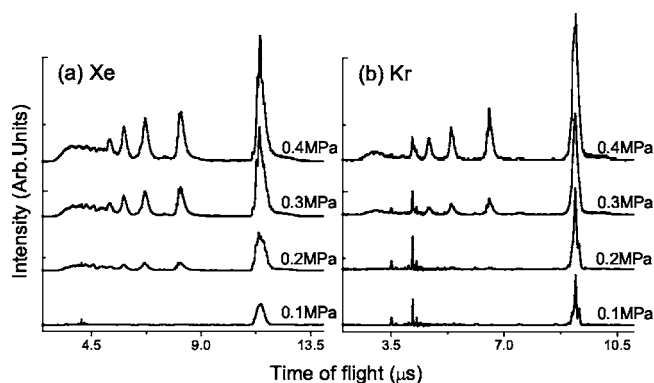


FIG. 3. Time-of-flight mass spectra of Xe and Kr clusters under different backing pressures. (a) Xe, gas pressures vary from 0.1 to 0.4 MPa, and (b) Kr, gas pressures vary from 0.1 to 0.4 MPa.

In order to know how the laser intensity affects the ratio and charge distribution of multicharged ions, TOF mass spectra were taken at different laser intensities in the range of  $(0.1-4) \times 10^{11} \text{ W cm}^{-2}$ , as shown in Fig. 4. From Fig. 4(a), we can see that the cluster assisted multiple ionization of xenon can take place even when the laser intensity is lowered to  $0.1 \times 10^{11} \text{ W cm}^{-2}$ , and the charge states of ions are not apparently decreased, while the total ion intensity is only about 0.5% of that of the maximal laser field. The threshold intensity needed to generate multicharged ions for krypton is  $0.5 \times 10^{11} \text{ W cm}^{-2}$ , which is almost 5 times higher than that for Xe, this is partially due to that MPI of the krypton atom needs one more 532 nm photon than the ionization of xenon.

We put forward an instructive mechanism herein, which is analogous to IIM proposed by Rose-Petruck *et al.* [14], to understand the generation of the highly charged ions at a laser power intensity as low as  $10^{10} \text{ W cm}^{-2}$ . The ionization events start from multiphoton ionization of atoms in neat xenon/krypton clusters, some of the MPI induced electrons can be caged inside a cluster due to (a) the rebound from collision with the solid-dense neutral atoms in the neighborhood, and (b) attraction of Coulomb ions cores. The caged electrons can be heated by the laser field through inverse

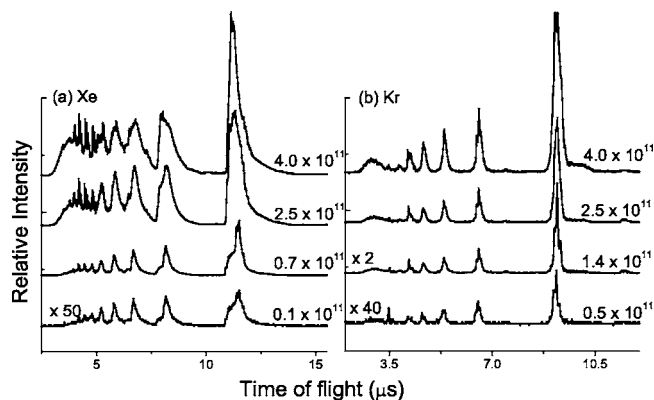


FIG. 4. Time-of-flight mass spectra of 0.4 MPa Xe and Kr clusters irradiated by different laser power densities at 532 nm, (a) Xe, laser intensities vary from  $4.0 \times 10^{11}$  to  $0.1 \times 10^{11} \text{ W cm}^{-2}$  and (b) Kr, laser intensities vary from  $4.0 \times 10^{11}$  to  $0.5 \times 10^{11} \text{ W cm}^{-2}$ .

bremsstrahlung (IBS) absorption when electrons collide with the neutrals or ions [23–25]. Once the electrons gain enough energy to surpass the corresponding ionization potential, EI ionization of neutral species, and recollide, multiple ionization of the ions would take place.

The average kinetic energy of an electron gained via IBS (disregarding the energy losses in the collisions) can be estimated from the following equation [15,23]:

$$\frac{d\varepsilon}{dt} = \Delta E \times \nu, \quad (1)$$

where  $\Delta E = 2U_p$  is the average energy absorbed by the electron in a single collision with an ion or neutral atom, and  $\nu$  is the collision frequency of electrons. For example,  $\Delta E$  is  $5.2 \times 10^{-4} \text{ eV}$  when a 532 nm laser with an intensity of  $0.1 \times 10^{11} \text{ W cm}^{-2}$  is used as the minimal laser intensity shown in Fig. 4. The average collision frequency of an electron with a neutral and ionized species inside the cluster is at the order of  $10^{14} \text{ s}^{-1}$ , as the total density of the species in the cluster is close to the density of the liquid of Xe or Kr, i.e.,  $10^{22} \text{ cm}^{-3}$ . The heating rate of an electron can reach 50–1000  $\text{eV ns}^{-1}$  at a laser intensity of  $10^{10}$ – $10^{11} \text{ W cm}^{-2}$ . So it takes only several hundreds of picoseconds to heat the electrons to sufficient kinetic energy to impact ionize the neutral atoms to ions, and recollide the ions to higher multicharged ions step by step. The ionization potentials of multicharged ions can be lowered due to ions and electrons in the proximity [2], which will enhance further EI ionization and produce more electrons around the ions. These heating and ionization processes circulate until the cluster explodes to pieces by increasing Coulomb-repelling forces.

According to the mechanism mentioned above, the differences between Figs. 2(a) and 2(b) could be understood. When a 532 nm laser irradiated on the middle portion of the jet beam, strong multicharged ions were observed in the mass spectra, while clusters excepting the  $\text{Xe}_2^+$  could hardly be found. When a 266 nm laser at intensity of around  $10^{11} \text{ W cm}^{-2}$  was used, there were much larger clusters in the mass spectra, together with very little high-charged ions. In fact the only appeared multicharged ion was  $\text{Xe}^{2+}$ . The ponderomotive potential  $U_p$  can be probably responsible for the appearance of the clusters and the disappearance of the very high-charged ions under a 266 nm laser field, which presents a linear relationship to the laser intensity and a square relationship to the laser wavelength. The  $U_p$  of a 266 nm laser is just about a quarter of that of a 532 nm laser, which results in a much more slower heating rate of the electron via IBS. The electrons caged in a cluster cannot gain enough kinetic energy to undertake further impact ionization to generate highly charged ions. Because of the absence of the highly charged ions and weak Coulomb-repelling forces in clusters, the larger clusters might have more opportunity to remain when irradiated by a 266 nm laser than by a 532 nm laser.

However, the real process in cluster-assisted multiple ionization is much more complicated, and the heating and ionizing of the cluster as well as the expanding are coexistent. The above analyses can bring us some qualitative conclusions: (1) A large cluster is absolutely vital for the generation

of the multicharged ions to restrict electrons within the clusters, enhance heating the electron, and promote EI ionization. (2) The heating of an electron in a cluster is very fast due to the near-solid density of the cluster, and the EI ionization process can take place very frequently to produce the very highly charged ions in the duration of nanosecond laser ionization. (3) The dominating process to produce multicharged ions is field ionization and enhanced field ionization in typical femtosecond experiments [1,2,11–15], and the relative strength of the electric field of the laser to the binding energy of the electron in an atom governs the final charge distribution of ions. While in nanosecond experiments, the kinetic energy of the electron gained via IBS governs the charge distribution, which increases linearly with the laser energy per pulse. The laser energy in the present experiment is about tens to hundreds of millijoules and is two orders larger than that used in the femtosecond experiment, this can account for that multicharged ions can be produced efficiently at laser intensities as low as  $10^{10}$  W cm<sup>-2</sup>.

#### IV. CONCLUSION

Cluster assisted production of highly charged xenon and krypton ions by a nanosecond laser ionization cluster have been reported in this work. An electron rescattering and recolliding ionization model is proposed to explain the ap-

pearances of those multiply charged clusters under low laser intensity of  $10^{10}$ – $10^{11}$  W cm<sup>-2</sup>, where the caged electron can gain its kinetic energy by inverse bremsstrahlung absorption from the laser field after multiphoton ionization. Several qualitative conclusions can be drawn out that: (1) A large cluster is completely essential for the production of the multicharged ions; (2) due to the fast heating rate of an electron in a cluster, an EI ionization process can take place very frequently to produce the highly charged ions; and (3) in nanosecond experiments, it is the kinetic energy of the electron that governs the charge distribution of multicharged ions, which is gained via IBS and increases linearly with the laser energy per pulse. The laser energy in the present experiment is about tens to hundreds of millijoules and is two orders larger than that used in general femtosecond experiments, this may be partially responsible for the efficient generation of multicharged ions at a laser intensity as low as  $10^{10}$  W cm<sup>-2</sup>.

#### ACKNOWLEDGMENTS

This work was partly supported by NSF of China and Center for Computational Science, Hefei Institutes of Physical Sciences. We would like to thank Professor Cunhao Zhang and Professor Guohe Sha for their instructive discussions.

- 
- [1] C. Siedschlag and Jan M. Rost, *Phys. Rev. Lett.* **93**, 043402 (2004).
  - [2] C. Siedschlag and Jan M. Rost, *Phys. Rev. A* **67**, 013404 (2003).
  - [3] S. Zamith, T. Martchenko, Y. Ni, S. A. Aseyev, H. G. Muller, and M. J. J. Vrakking, *Phys. Rev. A* **70**, 011201 (2004).
  - [4] M. B. Smirnov and V. P. Krainov, *Phys. Rev. A* **69**, 043201 (2004).
  - [5] E. Wells, I. Ben-Itzhak, and R. R. Jones, *Phys. Rev. Lett.* **93**, 023001 (2004).
  - [6] J. Rudati, J. L. Chaloupka, P. Agostini, K. C. Kulander, and L. F. DiMauro, *Phys. Rev. Lett.* **92**, 203001 (2004).
  - [7] H. Wabnitz, L. Bittner, A. R. B. de Castro, R. Döhrmann, P. Gürtler, T. Laarmann, W. Laasch, J. Schulz, A. Swiderski, K. von Haefen, T. Möller, B. Faatz, A. Fateev, J. Feldhaus, C. Gerth, U. Hahn, E. Saldin, E. Schneidmiller, K. Sytchev, K. Tiedtke, R. Treusch, and M. Yurkov, *Nature (London)* **420**, 482 (2002).
  - [8] A. Becker and F. H. M. Faisal, *Phys. Rev. A* **59**, R3182 (1999).
  - [9] K. Yamakawa, Y. Akahane, Y. Fududa, M. Aoyama, N. Inoue, H. Ueda, and T. Utsumi, *Phys. Rev. Lett.* **92**, 123001 (2004).
  - [10] E. M. Snyder, S. A. Buzza, and A. W. Castleman, Jr., *Phys. Rev. Lett.* **77**, 3347 (1996).
  - [11] I. Last and J. Jortner, *Phys. Rev. A* **60**, 2215 (1999).
  - [12] I. Last and J. Jortner, *Phys. Rev. A* **62**, 013201 (2000).
  - [13] I. Last and J. Jortner, *J. Chem. Phys.* **120**, 1348 (2004).
  - [14] C. Rose-Petruck, K. J. Schafer, K. R. Wilson, and C. P. J. Barty, *Phys. Rev. A* **55**, 1182 (1997).
  - [15] T. Ditmire, T. Donnelly, A. M. Rubenchik, R. W. Falcone, and M. D. Perry, *Phys. Rev. A* **53**, 3379 (1996).
  - [16] X. L. Kong, X. L. Luo, D. M. Niu, and H. Y. Li, *Chem. Phys. Lett.* **388**, 139 (2004).
  - [17] X. L. Luo, D. M. Niu, X. L. Kong, L. H. Wen, F. Liang, K. M. Pei, B. Wang, and H. Y. Li, *Chem. Phys.* **310**, 17 (2005).
  - [18] D. M. Niu, H. Y. Li, F. Liang, L. H. Wen, X. L. Luo, B. Wang, K. Y. Hou, and X. X. Zhang, *Chem. Phys. Lett.* **403**, 218 (2005).
  - [19] D. P. Armstrong, D. A. Harkins, R. N. Compton, and D. Ding, *J. Chem. Phys.* **100**, 28 (1994).
  - [20] M. Stuke, H. Reisler, and C. Witting, *Appl. Phys. Lett.* **39**, 201 (1981).
  - [21] M. A. Klossner and W. T. Silfvast, *Opt. Lett.* **23**, 1609 (1998).
  - [22] L. V. Keldysh, *Sov. Phys. JETP* **20**, 1307 (1965).
  - [23] J. E. Seely and E. G. Harris, *Phys. Rev. A* **7**, 1064 (1973).
  - [24] N. M. Kroll and K. M. Weston, *Phys. Rev. A* **8**, 804 (1973).
  - [25] Y. Shima and H. Yatom, *Phys. Rev. A* **12**, 2106 (1975).